Non-enzymatic electrochemical voltammetric sensors based on thulium:zinc oxide for dopamine detection

Dilber Esra Yıldız[1,*] , Fatma Unal[2], and Nevin Taşaltın[3,4,5,*]

[1] Department of Physics, Hitit University, Corum, Turkey

[2] Department of Biomedical Engineering, Samsun University, Samsun, Turkey

[3] Department of Basic Sciences, Maltepe University, Istanbul, Turkey

[4] Environmental and Energy Tech. Research Center, Maltepe University, Istanbul, Turkey

[5] CONSENS Inc, Maltepe University Research Center, Technopark Istanbul, Istanbul, Turkey

ABSTRACT

In this study, zinc oxide (ZnO) powders with dopant rates of 1 mol% thulium (Tm) (1Tm:ZnO), 2 mol% Tm (2Tm:ZnO), and 3 mol% Tm (3Tm:ZnO) nanoparticles were synthesized by co-precipitation method. Subsequently, Polyaniline (PANI)/1Tm:ZnO, PANI/2Tm:ZnO, and PANI/3Tm:ZnO nanocomposite sensors were prepared using a low-cost and simple sonication method. The results showed that the prepared PANI/1Tm:ZnO-based biosensor detected dopamine in the concentration range of (0.8–6.5) μM with a sensitivity of 0.2568 μAμM^{-1}cm^{-2}. Using these sensitivity values of the sensor, the LOD and LOQ values of the PANI/1Tm:ZnO-based sensor were calculated as 1.92 μM and 5.8 μM, respectively. The incorporation of 1% Tm into ZnO host (PANI/1Tm:ZnO) significantly enhanced the sensitivity of the biosensors.

1 Introduction

Electroanalytical methods are very useful for qualitative and quantitative analysis of physical, chemical, and biochemical systems, especially in nanotechnological applications. The chemical reaction characteristic of an analyte in an environment can be determined by electroanalytical methods depending on current and voltage. Electrochemical sensors are widely used in healthcare applications of sensors technology because it is easy, low-cost, and rapid to determine the chemical reaction characteristic of an analyte in the environment by electroanalytical methods. Electrochemical sensors provide the advantages such as easy to handle, low cost, and rapid response in healthcare applications [1–4]. Dopamine, glucose, uric acid, cholesterol in human blood can be determined using electrochemical sensors. Moreover, biomolecules can be detected in a few minutes with high sensitivity and good selectivity. Thus, early diagnosis of diseases caused by imbalances that occur due to the biomolecules in human blood being outside the lower and upper limits is facilitated [5–9].

Address correspondence to E-mail: desrayildiz@hitit.edu.tr; nevintasaltin@maltepe.edu.tr

Dopamine and glucose levels are crucial for human health. Dopamine is a neurotransmitter that plays a vital role in human and mammal systems, including the central nervous system, hormonal cardiovascular, and renal systems. It regulates behavior, mood, movement, memory, attention, cognition, pleasure, and hormonal processes. Dopamine imbalance can lead to neurological diseases such as Parkinson's disease, sleep and eating disorders, schizophrenia, attention-deficit hyperactivity disorder (ADHD), epilepsy, and senile dementia [10–15]. It also contributes to some diseases and drug addiction.

Enzymatic electrochemical biosensors were used to detect the dopamine and glucose, which are the source of several diseases. However, these sensors had limited use due to their instability, complicated enzyme purification procedure, easy loss of activity, complex immobilization procedure, short lifespan, high cost, and low sensitivity due to indirect electron transfer [16–23]. It also had limited stability and poor reproducibility as it was prone to enzyme activity, limited temperature, pH, humidity, and toxic chemicals. Furthermore, enzymes could not be implanted in the human body for a long time due to their rapid degradation [21–23]. In the last two decades, scientists have turned to non-enzymatic electrochemical sensors to overcome the limitations of enzymatic electrochemical sensors. These sensors have significant advantages such as high sensitivity, long-term stability, low cost, large-scale production, and excellent reproducibility [22, 24–30, 25, 24]. ZnO, NiO, CuO, Co_3O_4, MgO, TiO_2, IrO_2, and SnO_2 metal oxides were used as an enzymatic electrochemical sensors [22, 31–37]. Among these, ZnO powders have unique properties such as ease of manufacture, non-toxicity, high chemical stability, electrochemical activity, optical and electrical properties, high electrocatalytic activity, high loading capacity, biocompatibility, and high electron transfer properties, making them an attractive option [17, 23, 38, 39].

Recent researches have shown that doping rare-earth ions to ZnO powders provides sensors with fast oxygen ion mobility and high surface basicity, improving their chemical interactions and sensing capabilities by changing the structural and morphological properties of the host material [40–43]. There are limited studies on lanthanide-doped non-enzymatic electrochemical biosensors for dopamine and glucose applications in the literature [41–43]. In this study, PANI/Tm-doped ZnO biosensors for dopamine detection applications were produced, and the effect of Tm rare-earth dopant element amount on biosensor properties was investigated for the first time.

2 Experimental

Zinc nitrate hexahydrate ($Zn(NO_3)_2 \times 6H_2O$, 99%) (Sigma-Aldrich), thulium nitrate hydrate ($Tm(NO_3)_3.\times H_2O$, 99.9%) (Alfa Aesar), and ammonium carbonate (($NH_4)_2CO_3$, 99.9%) were used as starting materials for the production of Tm-doped ZnO particles via co-precipitation method. Initially, determined stoichiometric amounts of zinc nitrate and thulium nitrate salts were dissolved in 150 ml of distilled water (DI) and, stirred at the speed of 400 rpm at ambient conditions for 30 min to obtain first solution. At the same time, 1 M ammonium carbonate solution was prepared to obtain second solution. The second solution was slowly dropped into the first solution until the pH of solution reached ∼ 10.

Upon addition of the ammonium carbonate solution (second solution), white precipitates began to form and, this solution was stirred for 2 h to complete the reaction. The obtained white solutions were thoroughly washed with DI and ethanol by centrifugation at 4000 rpm for 10 min. It was dried in an oven at 80 °C under ambient conditions. Finally, the dried powders were ground and heat treated at 850 °C for 3 h using sintered alumina crucible to produce Tm-doped ZnO particles. 1 mol%, 2 mol%, and 3 mol% Tm-doped ZnO nanoparticles were coded as 1Tm:ZnO, 2Tm:ZnO, and 3Tm:ZnO, respectively.

The gold transducers with gold (Au) thin-film electrode on printed circuit board (PCB) were purchased from Ebtro Electronics (Turkey), and ultra-pure DI with a resistance of 18.2 MΩ (Human Corporation) was used. FTIR and SEM analysis were performed at TUBITAK Marmara Research Center, Turkey. The FTIR spectra of conducting polymer blends were measured by dispersing them in KBr pellets using a Varian 1000 FTIR Spectrometer. Surface characterization studies were conducted using scanning electron microscopy (SEM) (Hitachi SU 1510, Japan). All electrochemical measurements were conducted under ambient conditions (25 °C) using a potentiostat (Ebtro Electronics).

Polyaniline (PANI) and N-methyl pyrrolidone (NMP) were purchased from Sigma-Aldrich and Merck, respectively. To obtain polyaniline

(PANI) nanocomposites such as PANI/1Tm:ZnO, PANI/2Tm:ZnO, and PANI/3Tm:ZnO nanocomposites, 1 mg of 1Tm:ZnO, 2Tm:ZnO, and 3Tm:ZnO nanoparticles were separately mixed in 2 ml NMP, respectively, and all solutions were sonicated for 5 min. The gold transducers were cleaned using ethanol, and then the prepared nanocomposites were drop casted on the gold transducers and dried at 40 °C to obtain non-enzymatic sensors. Phosphate buffer saline (PBS) tablet was purchased from Sigma-Aldrich (product code 79,382). The responses of the sensors were tested against dopamine concentration in PBS. Current–Voltage (I–V) characteristics of the sensors were obtained by applying (− 1, + 1)V with 50 mV/s scan rate at 25 °C. The limit of detection (LOD) values of the sensors were calculated using their sensitivity values.

3 Results and discussion

The morphology of the prepared PANI/1Tm:ZnO, PANI/2Tm:ZnO, and PANI/3Tm:ZnO nanocomposites was investigated using Scanning Electron Microscopy (SEM) (Fig. 1). PANI/Tm:ZnO nanocomposites showed a different surface morphology with aggregates due to the existence of Tm-doped ZnO nanoparticles within the PANI matrix. PANI/1Tm:ZnO nanocomposites exhibited irregular nearly spherical morphology. However, PANI/2Tm:ZnO nanocomposites revealed flake-shaped morphology, while PANI/3Tm:ZnO nanocomposites demonstrated a network structure.

In order to examine the molecular bonding characteristics of PANI/Tm:ZnO nanocomposites, Fourier Transform Infrared Spectroscopy Analysis (FTIR) was performed using Varian 1000 FTIR Spectrometer device. The FTIR spectra were acquired in 4000–400 cm^{-1} range under ambient conditions and are given in Fig. 2. Absorption bands of nanocomposites at 498, 647, 707, 742, 823, 957, 1160, 1241, 1292, 1381, 1496, 1581, 1659, 2849, 2918, and around 3200 cm^{-1} were observed. The peaks at 498, 647, and 707 cm^{-1} were due to the stretching modes of metal oxygen bonds ((Zn,Tm)–O) [44–47]. The absorption peak at 742 cm^{-1} was attributed C–H bonding mode [48]. The absorption peak at 823 cm^{-1} confirms the characteristic of paradisubstituted aromatic rings in which the polymerization progresses in all polymers [49]. The absorption peaks at 957 and 1160 cm^{-1} were ascribed to C–H bending vibrational modes [50]. The

characteristic absorption peaks at 1241 and 1292 cm^{-1} were associated to C–H and C–N bending modes of benzenoid and quinoid rings, confirming the successful synthesis of PANI [51]. The absorption peak at 1381 cm^{-1} corresponded to C–N stretching modes in the neighborhood of a quinoid ring [52]. The absorption peaks at 1496 and 1581 cm^{-1} were attributed to C=C and C=N and stretching vibrations of quinone and benzene rings, respectively [53]. The absorption peaks at 1659, 2849, and 2918 cm^{-1} were ascribed to C=O, C–H, and N–H vibration modes, respectively [43, 54, 55]. Additionally, the broad band at 3200 cm^{-1} indicated O–H stretching modes [56].

The schematic representations of sensing mechanism of PANI/1Tm:ZnO nanocomposite, PANI/2Tm:ZnO nanocomposite, and PANI/3Tm:ZnO nanocomposite-based non-enzymatic electrochemical sensors against dopamine are given in Fig. 3. As seen in Fig. 3, dopamine was oxidized by LAC (oxidized) to fabricate the dopamine-o-quinone (DOQ), and then LAC (reduced) eliminated the electrons to constitute LAC (oxidized). For that reason, after an electrocatalytic cycle, electrons were transferred to the working electrodes [57, 58]. In this study, it was fabricated a novel PANI/Tm:ZnO nanocomposites electron transfer sensor for dopamine detection, based on the fact that dopamine can decrease Tm^{+} ion to nanoparticles followed by oxidized to DOQ.

Electrochemical measurements were carried out to detect dopamine at concentrations ranging from 0.8 to 6.5 μM for three different sensors (PANI/1Tm:ZnO, PANI/2Tm:ZnO, and PANI/3Tm:ZnO-coded nanocomposites). The current density–voltage curves of each sensor were plotted for all concentrations, and the peak values of current densities versus dopamine concentrations were also recorded. The sensitivity values of the sensors were obtained from the slope of the curves, as shown in Fig. 4. The PANI/1Tm:ZnO-based sensor (Fig. 4a) exhibited two prominent current density peaks in voltammetry measurements, resulting from redox reactions of dopamine. However, PANI/2Tm:ZnO-based sensor (Fig. 4b) and PANI/3Tm:ZnO-based sensor (Fig. 4c) did not exhibit any significant current density peaks against dopamine. The peak values of the current densities decreased with the decrease in dopamine concentration. The sensor was able to detect dopamine in the concentration range of 0.8 to 6.5 μM with a sensitivity of 0.2568 $μAμM^{-1} cm^{-2}$ (Fig. 4d). Using the sensitivity values of the sensor, the Limit of Detection (LOD)
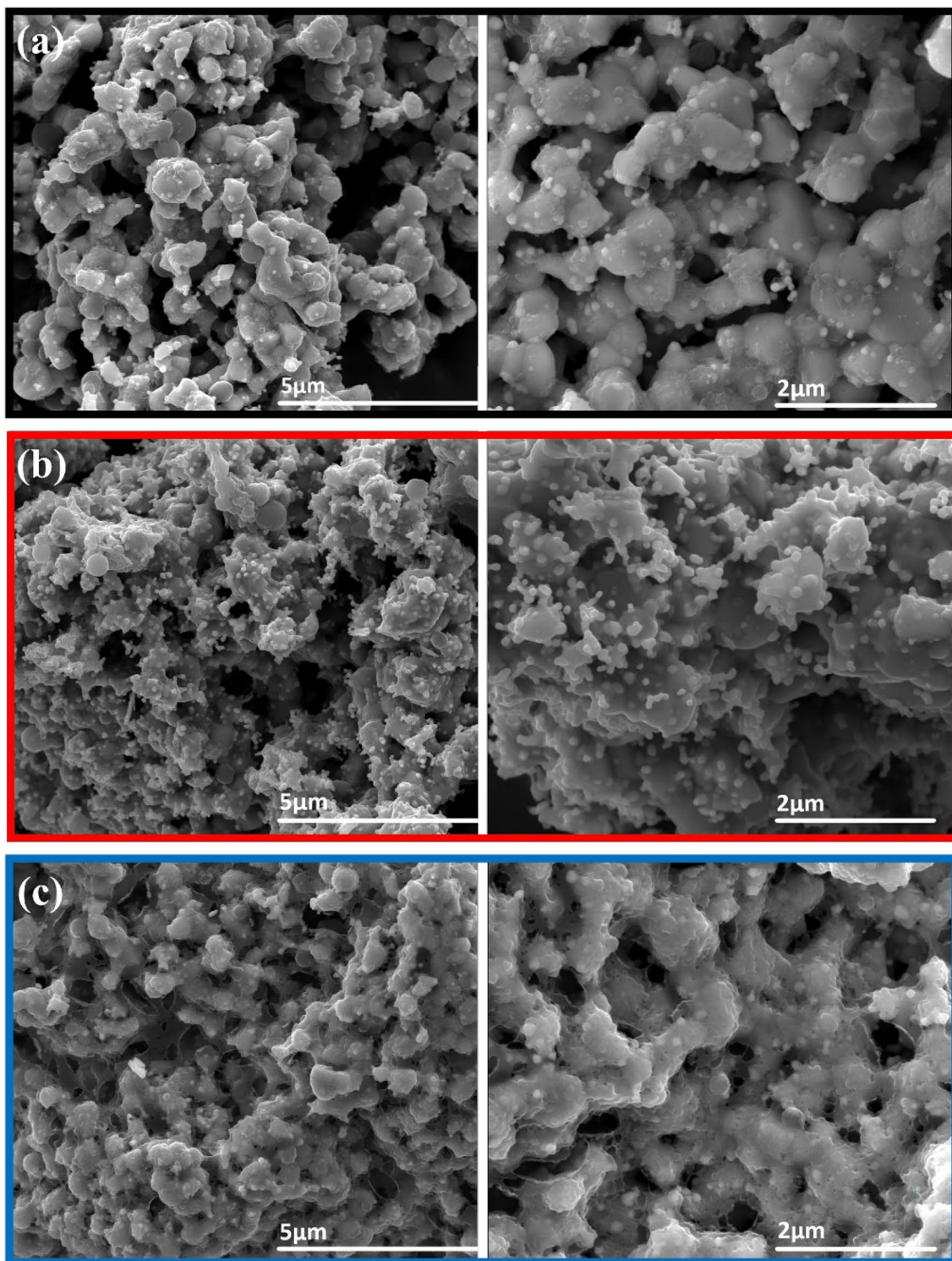
Fig. 1 SEM images of the prepared **a** PANI/1Tm:ZnO nanocomposite, **b** PANI/2Tm:ZnO nanocomposite, and **c** PANI/3Tm:ZnO nanocomposite

and Limit of Quantification (LOQ) values for the PANI/1Tm:ZnO-based sensor were calculated as 1.92 μM and 5.8 μM, respectively. The sensor tests were repeated 4 times, and all the sensor results were identical to the each other. PANI/1Tm:ZnO-based sensor is
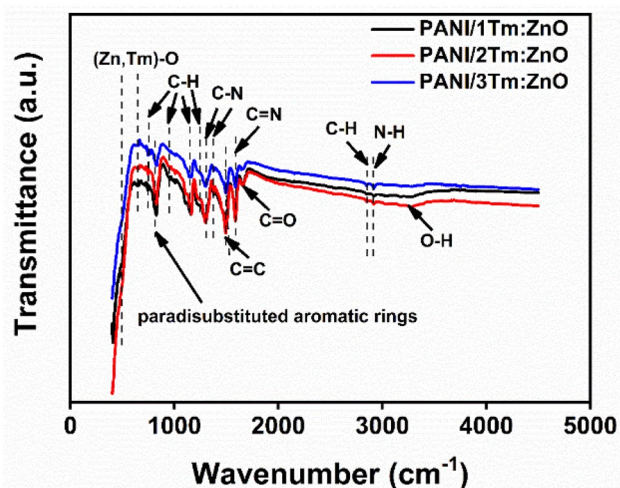
Fig. 2 FTIR spectra of the prepared PANI/1Tm:ZnO nanocomposite, PANI/2Tm:ZnO nanocomposite, and PANI/3Tm:ZnO nanocomposite

a potential device for rapid, low-cost, sensitive, and stable for detection of dopamine.

As known, electrical conductivity (σ) and impedance (Z) are interrelated parameters in devices such as solar cells, sensors, and photodiodes and directly affect the current–voltage characteristics of the device [59–63]. For this reason, all materials such as PANI, 1Tm:ZnO, 2Tm:ZnO, 3Tm:ZnO, dopamine, and dopamine concentration (0.81–6.5 µM) used in a biosensor contribute to the Z, σ, and conductance (G) of the biosensors and they directly affect the biosensor's current density–voltage (J–V) curves of PANI/1Tm:ZnO-based sensor, PANI/2Tm:ZnO-based sensor, and PANI/3Tm:ZnO ZnO-based sensor (Fig. 2). Therefore, G and Z of all biosensors are investigated for these biosensors. In addition, the σ value is a material constant and varies only depending on the material (like PANI or PANI/1Tm:ZnO), while the G and Z values
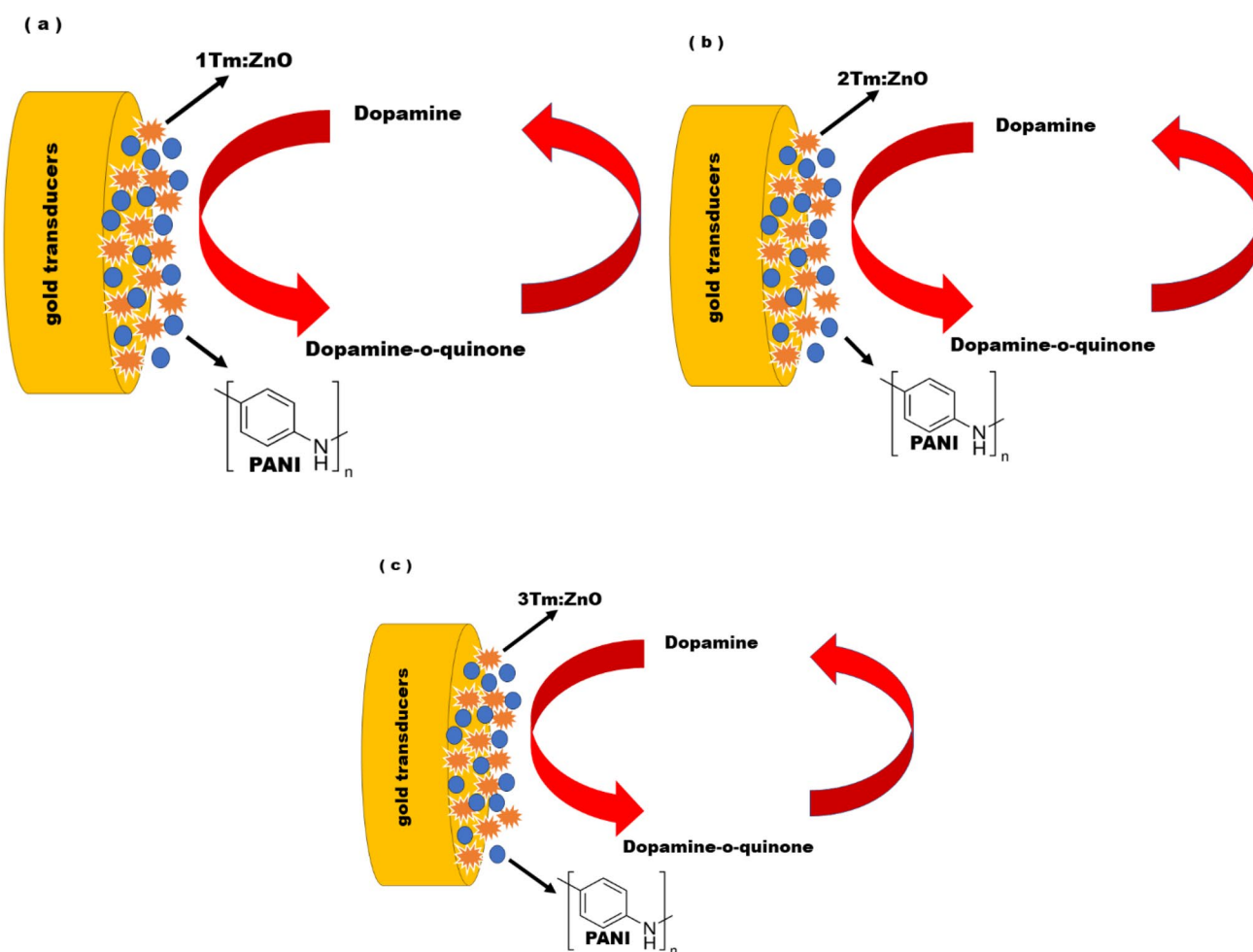

Fig. 3 The schematic representations of sensing mechanism of **a** PANI/1Tm:ZnO nanocomposite, **b** PANI/2Tm:ZnO nanocomposite, and **c** PANI/3Tm:ZnO nanocomposite-based non-enzymatic electrochemical sensors against dopamine
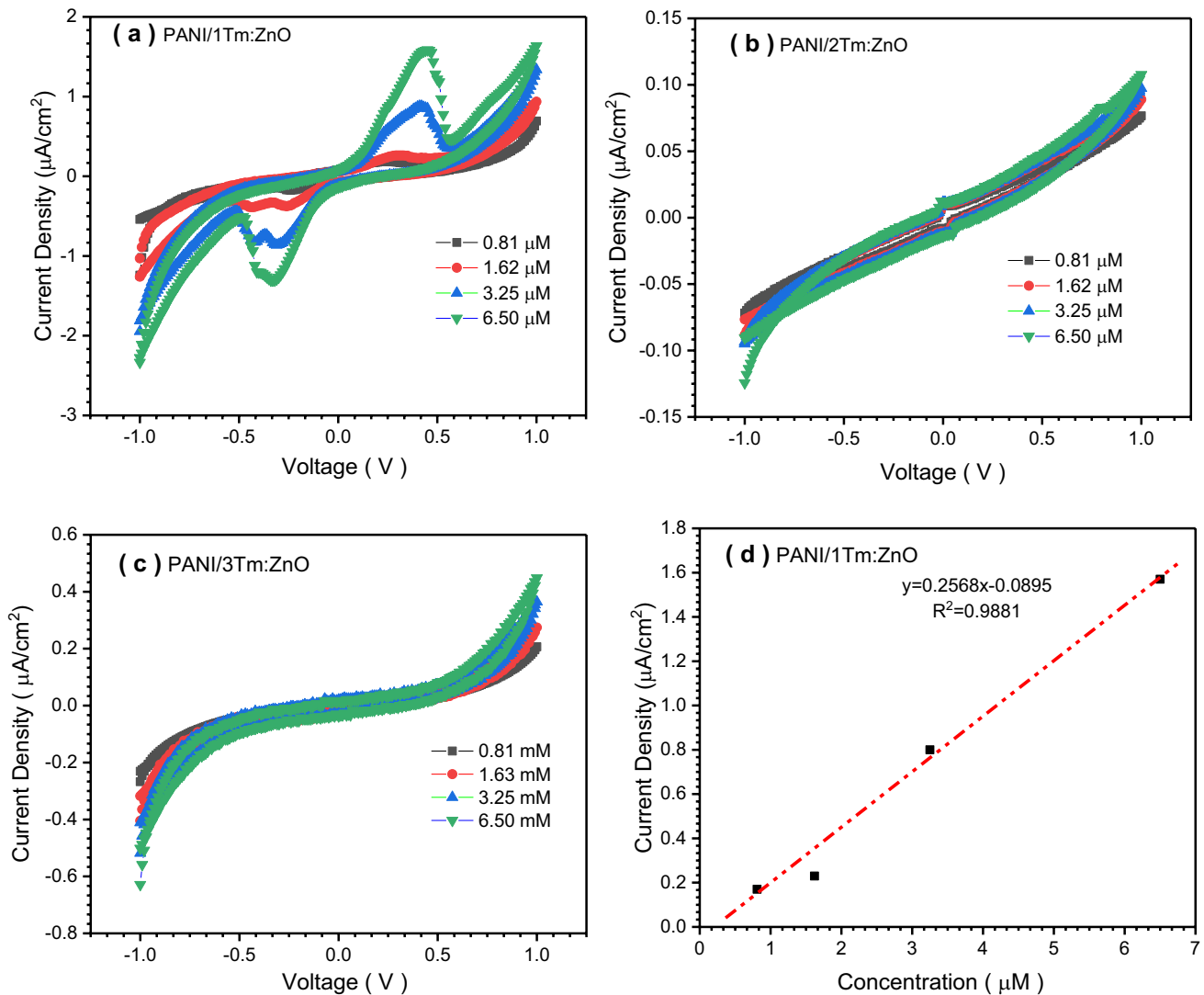
Fig. 4 The current density–voltage curves of **a** PANI/1Tm:ZnO-based sensor, **b** PANI/2Tm:ZnO-based sensor, **c** PANI/3Tm:ZnO-based sensor, and **d** the sensitivity of the PANI/1Tm:ZnO-based sensor against dopamine

depend on the properties of a particular device (like a biosensor).

Mathematically, in the $G = \sigma A/L$ formula A (cm^2), L (cm), G (S), and σ (Scm^{-1}) represent the cross-sectional area, its length, the conductance, and the conductivity, respecitvely [59]. As seen in the formula, σ is closely related to G. Similar relationships can be found between G and Z or Z of biosensors and current density. The G is the inverse of resistance (Z'), meaning that it is a measure of how easily current will flow through the material. As seen Figs. 2 and 4, the dopamine concentration is affected by the biosensor's current density–voltage curves, the impedance, and conductance of these biosensors.

The $Z = Z' + iZ''$ where Z, Z'' and Z' represent complex impedance, the imaginary and real parts, respectively [62–65]. The inverse of conductivity is reel part of empedans. The Z and conductance (G) values of PANI/1Tm:ZnO, PANI/2Tm:ZnO, and PANI/3Tm:ZnO-based sensors taken at various dopamine concentrations at 0.8 V are given in Fig. 5. As seen in Fig. 5, the Z and G values of all sensors are inversely proportional to the each other, and as the G value increases, the Z value decreases with the increase in dopamine concentration. Also, while the G values of PANI/1Tm:ZnO-based sensors are higher than PANI/2Tm:ZnO and PANI:3Tm-based sensors, the Z value of PANI/1Tm:ZnO-based sensors is
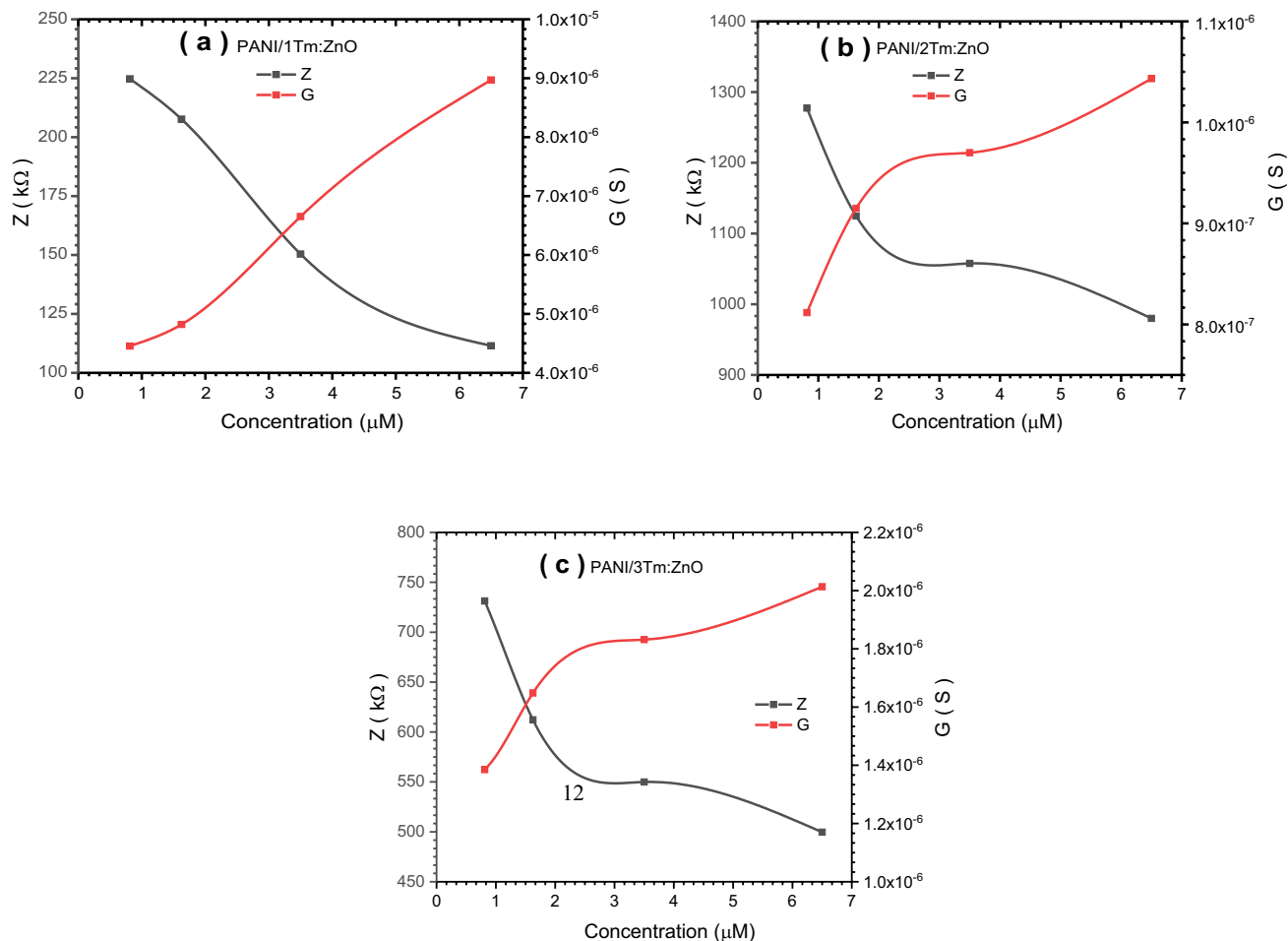
Fig. 5 The Z and G values of **a** PANI/1Tm:ZnO, **b** PANI/2Tm:ZnO, and **c** PANI/3Tm:ZnO-based sensor at 0.6 V

Table 1 The Z and G values of PANI/1Tm:ZnO, PANI/2Tm:ZnO, and PANI/3Tm:ZnO sensors

Dopamine concentration (μM)	PANI/1Tm:ZnO		PANI/2Tm:ZnO		PANI/3Tm:ZnO	
	Z (kΩ)	G (S)	Z (kΩ)	G (S)	Z (kΩ)	G (S)
0.8125	2.25×10^2	4.46×10^{-6}	1.28×10^3	8.12×10^{-7}	7.31×10^2	1.39×10^{-6}
1.625	2.08×10^2	4.82×10^{-6}	1.12×10^3	9.15×10^{-7}	6.12×10^2	1.65×10^{-6}
3.5	1.50×10^2	6.65×10^{-6}	1.06×10^3	9.7×10^{-7}	5.50×10^2	1.83×10^{-6}
6.5	$\mathbf{1.11\times10^2}$	$\mathbf{8.97\times10^{-6}}$	9.80×10^2	1.04×10^{-6}	5.00×10^2	2.01×10^{-6}

lower than other sensors. As seen in Table 1, the G value for PANI/1Tm:ZnO-based sensor is 8.97×10^{-6} S and the Z value for PANI/1Tm:ZnO-based sensor is 1.11×10^2 kΩ at 6.5 μM. Tm dopant amount in ZnO host was not observed to cause a proportional increase in impedance of PANI/1Tm:ZnO-based sensor, PANI/2Tm:ZnO-based sensor, and PANI/3Tm:ZnO-based sensor. The impedance values of the PANI:2Tm:ZnO biosensor were the highest compared to other biosensors, and these values decreased with increasing dopamine concentration (0.81–6.5 μM). Also, the impedance values of the PANI:1Tm:ZnO biosensor were the lowest compared to other biosensors, and these values decreased with increasing dopamine concentration (0.81–6.5 μM). Similarly, Tm dopant amount in ZnO was not observed to lead to a proportional increase in conductance. The conductance values of the PANI:1Tm:ZnO biosensor were the highest

and these values increased with increasing dopamine concentration (0.81–6.5 mM). Z and G values of the PANI/1Tm:ZnO biosensor taken at 6.5 μM dopamine concentration are bolded in Table 1.

The Nyquist plots (Z″ vs. Z′ plot) of PANI/1Tm:ZnO, PANI/2Tm:ZnO, and PANI/3Tm:ZnO biosensors were obtained based on the frequency range from 1 to 100 kHz. As seen in Fig. 6, Z″and Z′ values increased with decreasing frequency [66–69]. The behavior of Z′ increased with decreasing frequency owing to the space-charge polarization in PANI/1Tm:ZnO, PANI/2Tm:ZnO, and PANI/3Tm:ZnO-based sensor [70–76]. Also, the Z′ values of PANI/2Tm:ZnO and PANI/3Tm:ZnO nanocomposites were higher than that of Z′ for PANI/1Tm:ZnO. Similarly, the value of the Z″ for PANI/1Tm:ZnO-based sensors was smaller than the others. Consequently, the impedance and conductance results were compatible with each other and were an effective parameter in the sensitivity and current density of the sensors. When the conductivity of the biosensor increases, the conductance increases and the impedance decreases. As a result, the current response of the sensor will increase, and the high sensitivity of the biosensors will be associated with these results.

L. Yang et al. [42] fabricated AuNPs@PANI core/shell nanocomposite-based electrochemical sensor and tested the sensor against dopamine between 10 and 1700 μM using cyclic voltammetry method. The LOD of the sensor was found to be 5 μM. C. Ratlam et al. [77] prepared PANI and PANI/CQDs film-based electrochemical sensors and tested them against dopamine in the range of 10–90 μM using cyclic voltammetry method. LOD values of them were 0.2089 μM and 0.1013 μM, respectively. Sensitivity values of them were $7.587\ nA\mu M^{-1}cm^{-2}$ and $8.025\ nA\mu M^{-1}cm^{-2}$, respectively. W.-F. Hsu et al. [78] produced SnO_2/PANI/N-GQD-based electrochemical sensor and tested the sensor via differential pulse voltammetry method against dopamine in the range of 0.5–200 μM. They found that LOD of the sensor was 0.22 μM. L.-Q. Xie et al. [79] prepared PANI/rGO/Nafion nanocomposite-based electrochemical sensor and tested the sensor against dopamine in the range of 0.05–60.0 mmol/L using differential pulse voltammetry method. LOD of the sensor was detected to be 0.024 mmol/L. J. Mathiyarasu [80] prepared PANI boronic acid-modified glassy carbon electrode and tested the sensor using differential pulse voltammetry method in the range of 0.005–0.2 mM dopamine concentration. Sensitivity
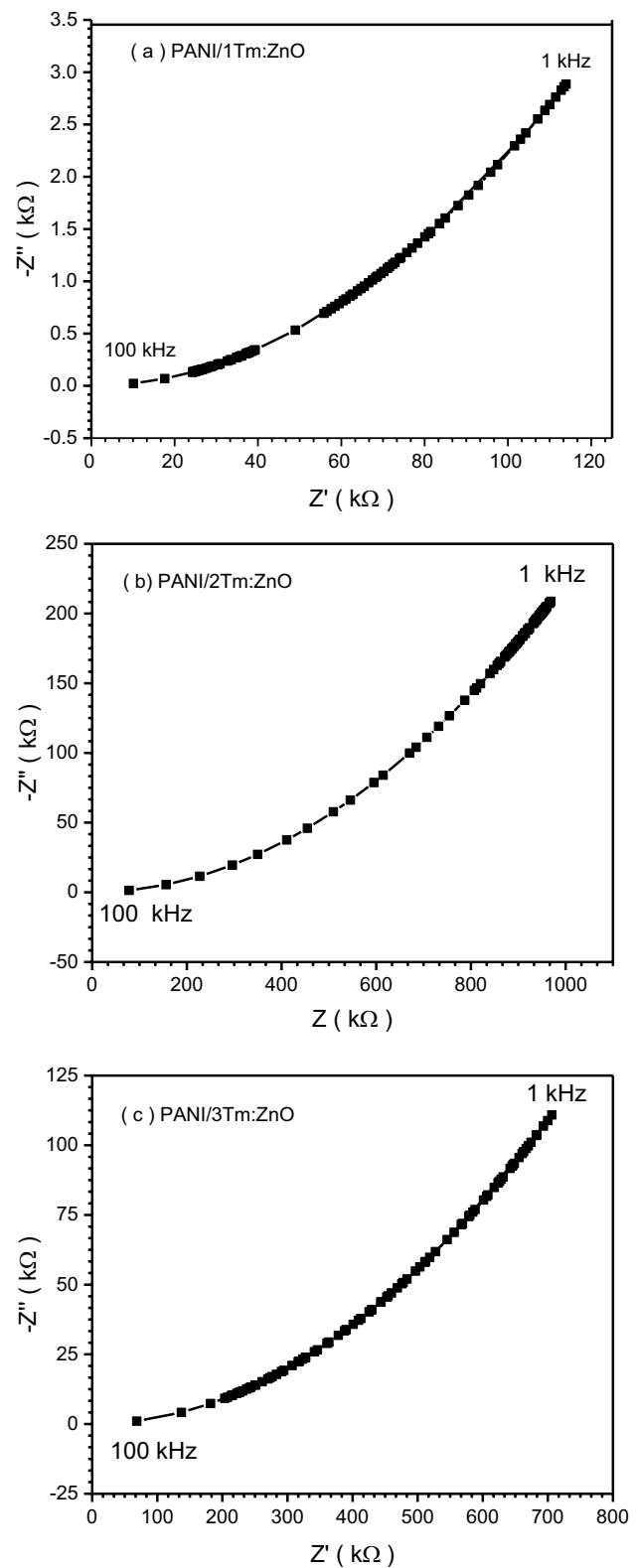

Fig. 6 Typical Nyquist plots of **a** PANI/1Tm:ZnO, **b** PANI/2Tm:ZnO, and **c** PANI/3Tm:ZnO-based sensors

Table 2 The comparison of this study with the previous studies

Electrode material	Sensitivity	LOD	Linear range	References
PANI	7.587 nAμM^{-1}cm^{-2}	0.2089 μM	10–90 μM	[77]
PANI/CQDs film	8.025 nAμM^{-1}cm^{-2}	0.1013 μM	–	[77]
AuNPs@PANI coreshell nanocomposite	–	5 μM	10–1700 μM	[43]
SnO$_2$/PANI/N-GQD	–	0.22 μM	0.5–200 μM	[78]
PANI/rGO/Nafion nanocomposite	–	0.024 mmol/L	0.05–60.0 mmol/L	[79]
PANI boronic acid-modified glassy carbon electrode	0.02 μAμM^{-1}	–	0.005–0.2 mM	[80]
PANI/1Tm: ZnO	0.2568 μAμM^{-1} cm^{-2}	1.92 μM	0.8–6.5 μM	This study

of the sensor was 0.02 μAμM^{-1}. In this study based on these studies, the sensitivity and LOD values of the PANI/1Tm:ZnO-based electrochemical sensor showed remarkably good performance in the low dopamine concentration range. The comparison of this study with previous studies iss given in Table 2.

4 Conclusion

PANI/1Tm:ZnO nanocomposites, as a new material obtained after mixing PANI with Tm-doped ZnO nanoparticles, exhibited a more individual and smooth morphology compared to other nanocomposites. Other nanocomposites exhibited more aggregation and a network-like morphology after the same nanocomposite preparation process. The uniform morphology of the PANI/1Tm:ZnO nanocomposites enabled this new nanostructure to detect dopamine with increasing linear sensitivity at uniform concentrations. This biosensor, which has the potential to be used as a dopamine sensor in personal biomedical devices, can detect 1.92 μM dopamine in a 1-minute voltammetric cycle. Also, the impedance and conductance results are compatible with each other and are effective parameters in the sensitivity and current density of sensors. It is clearly that the high sensitivity of sensors correlate to conductance, conductivity, and impedance of devices. As a result, while the G values of PANI/1Tm:ZnO-based sensors are higher than that of PANI/2Tm:ZnO and PANI/3Tm:ZnO-based sensors, the Z value of PANI/1Tm:ZnO-based sensors is lower than the other sensors.

Author contributions

DEY: Investigation, Methodology, Writing—Review and Editing, Funding, Supervision. FU: Investigation, Methodology, Writing—Review and Editing NT: Investigation, Writing—Review and Editing, Methodology, Funding.

Data availability

The datasets generated during and/or analyzed during the current study are available from the corresponding author upon reasonable request.

Declarations

Conflict of interest The authors declare that they have no conflict of interest.

References

1. H.S. Nejad, F.G. Nejad, H. Beitollahi, Development of a highly sensitive voltammetric sensor for the detection of folic acid by using MoS2 and ionic liquid-modified carbon paste electrode. ADMET and DMPK **11**(3), 361–371 (2023)

2. F. Beigmoradi, H. Beitollahi, Fe_3O_4/GO nanocomposite modified glassy carbon electrode as a novel voltammetric sensor for determination of bisphenol A. J. Electrochem. Sci. Eng. **12**(6), 1205–1214 (2022)

3. H. Beitollahi, S. Tajik, M.R. Aflatoonian, A. Makarem, Glutathione detection at carbon paste electrode modified with ethyl 2-(4-ferrocenyl-[1, 2, 3] triazol-1-yl) acetate, ZnFe2O4 nano-particles and ionic liquid. J. Electrochem. Sci. Eng. **12**(1), 209–217 (2022)

4. H. Beitollahi, S. Tajik, M.R. Aflatoonian, A. Makarem, A sensitive Cu (salophen) modified screen-printed electrode for simultaneous determination of dopamine and uric acid. J. Electrochem. Sci. Eng. **12**(1), 199–208 (2022)

5. G.A. Mohammadi, H. Beitollahi, I. Sheikhshoaie, S. Tajik, M.R. Aflatoonian, An electrochemical sensing platform based on Fe3O4@ CuO core-shell nanocomposite modified screen printed graphite electrode for sensitive hydroxylamine detection. Int. J. Environ. Anal. Chem. **103**(19), 7773–7787 (2023)

6. G.A. Mohammadi, I. Sheikhshoaie, H. Beitollahi, M.R. Aflatoonian, S. Tajik, A reliable electrochemical approach for detection of sulphite with Tl-doped in Mn3O4 nanostructures and ionic liquid-modified carbon paste electrode. Int. J. Environ. Anal. Chem. **103**(18), 6526–6538 (2023)

7. A. Mikhraliieva, V. Zaitsev, O. Tkachenko, M. Nazarkovsky, Y. Xing, E.V. Benvenutti, Graphene oxide quantum dots immobilized on mesoporous silica: preparation, characterization and electroanalytical application. RSC Adv. **10**(52), 31305–31315 (2020)

8. H. Beitollahi, M. Safaei, S. Tajik, Different electrochemical sensors for determination of dopamine as neurotransmitter in mixed and clinical samples: a review. Anal. Bioanalytical Chem. Res. **6**(1), 81–96 (2019)

9. S. Tajik, M.A. Taher, H. Beitollahi, The first electrochemical sensor for determination of mangiferin based on an ionic liquid–graphene nanosheets paste electrode. Ionics **20**, 1155–1161 (2014)

10. R.M. Wightman, L.J. May, A.C. Michael, Detection of dopamine dyanamic in the brain. Anal. Chem. **60**(13), 769A-793A (1988)

11. K.M. Biglan, R.G. Holloway, A review of pramipexole and its clinical utility in Parkinson's disease. Expert Opin. Pharmacother. **3**(2), 197–210 (2005)

12. K.Y. Tsai, H.F. Peng, J.J. Huang, Nafion modified electrochemical sensor integrated with a feedback-loop indium-gallium-zinc oxide thin-film transistor for enhancing dopamine detection limit. Sens. Actuators Phys. **354**, 114287 (2023)

13. G. Venkataprasad, T. Madhusudana Reddy, A. Lakshmi Narayana, O.M. Hussain, P. Shaikshavali, T. Venu Gopal, P. Gopal, A facile synthesis of Fe_3O_4-Gr nanocomposite and its effective use as electrochemical sensor for the determination of dopamine and as anode material in lithium ion batteries. Sens. Actuators Phys. **293**, 87–100 (2019)

14. A.L. Narayana, G. Venkataprasad, S. Praveen, C.W. Ho, H.K. Kim, T.M. Reddy, C.M. Julien, C.W. Lee, Li_2TiO_3-MWCNT nanocomposite electrodes for determination of dopamine in electrochemical sensing platform. Sens. Actuators Phys. **341**, 113555 (2022)

15. J.W. Oh, Y.W. Yoon, J. Heo, J. Yu, H. Kim, T.H. Kim, Electrochemical detection of nanomolar dopamine in the presence of neurophysiological concentration of ascorbic acid and uric acid using charge-coated carbon nanotubes via facile and green preparation. Talanta. **147**, 453–459 (2016)

16. R. Ahmad, M. S. Ahn, Y. B. Hahn, Fabrication of a non-enzymatic glucose sensor field-effect transistor based on vertically-oriented ZnO nanorods modified with Fe_2O_3. Electrochem. Commun. **77**, 107–111 (2017)

17. R. Ahmad, N. Tripathy, M.-S. Ahn, K. S. Bhat, T. Mahmoudi, Y. Wang, J.-Y. Yoo, D.-W. Kwon, H.-Y. Yang, Y.-B. Hahn, Highly efficient non-enzymatic glucose sensor based on CuO modified vertically-grown ZnO nanorods on electrode. Sci. Rep. **7**, 5715 (2017)

18. S. Joshi, V.D. Bhatt, A. Märtl, M. Becherer, P. Lugli, Regenerative, highly-sensitive, non-enzymatic dopamine

sensor and impact of different buffer systems in dopamine sensing. Biosensors. **8**, 9 (2018)

19. C. Bavatharani, E. Muthusankar, Z.A. Alothman, S.M. Wabaidur, V.K. Ponnusamy, D. Ragupathy, Ultra-high sensitive, selective, non-enzymatic dopamine sensor based on electrochemically active graphene decorated Polydiphenylamine-SiO_2 nanohybrid composite. Ceram. Int. **46**, 23276–23281 (2020)

20. H.Y. Yue, H.J. Zhang, S. Huang, X. Gao, S.S. Song, Z. Wang, W. Q. Wang, E. H. Guan, A novel non-enzymatic dopamine sensors based on NiO-reduced graphene oxide hybrid nanosheets. J. Mater. Sci. Mater. Electron. **30**, 5000–5007 (2019)

21. A. Mahmoud, M. Echabaane, K. Omri, L. El Mir, R.B. Chaabane, Development of an impedimetric non enzymatic sensor based on ZnO and Cu doped ZnO nanoparticles for the detection of glucose. J. Alloys Compd. **786**, 960–968 (2019)

22. A. El Golli, M. Echabaane, C. Dridi, Development of an electrochemical nanoplatform for non-enzymatic glucose sensing based on Cu/ZnO nanocomposite. Mater. Chem. Phys. **280**, 125844 (2022)

23. Y. Yang, Y. Wang, X. Bao, H. Li, Electrochemical deposition of Ni nanoparticles decorated ZnO hexagonal prisms as an effective platform for non-enzymatic detection of glucose. J. Electroanal. Chem. **775**, 163–170 (2016)

24. G. Wang, X. He, L. Wang, A. Gu, Y. Huang, B. Fang, B. Geng, X. Zhang, Received: non-enzymatic electrochemical sensing of glucose. Microchim. Acta. **180**, 161–186 (2013)

25. K.E. Toghill, R.G. Compton, Basic potential step methods, electrochemical non-enzymatic glucose sensors: a perspective and an evaluation. Int. J. Electrochem. Sci. **5**, 1246–1301 (2010)

26. M.H. Hassan, C. Vyas, B. Grieve, P. Bartol, Recent advances in enzymatic and non-enzymatic electrochemical glucose sensing. Sensors. **21**, 4672 (2021)

27. G. Balkourani, T. Damartzis, A. Brouzgou, P. Tsiakaras, Cost effective synthesis of graphene nanomaterials for comprehensive review. Biosens. Sensors. **22**, 355 (2022)

28. H. Yang, C. Zhou, J. An, L. Yang, Y. Yang, X. Liu, Ultra-fast synthesis of iron decorated multiwalled carbon nanotube composite materials: a sensitive electrochemical sensor for determining dopamine. J. Alloys Compd. **897**, 163257 (2022)

29. A.V. Ambika, N. Navya, H.N. Sumedha, S.R.K. Kumar, B.L. Suresha, Electrochemical sensor studies of dopamine using multiwalled carbon nanotubes by CVD technique. Phys. B Condens. Matter. **620**, 413137 (2021)

30. M. Ni, J. Chen, C. Wang, Y. Wang, L. Huang, W. Xiong, P. Zhao, Y. Xie, J. Fei, A high-sensitive dopamine

31. S. Liu, B. Yu, T. Zhang, A novel non-enzymatic glucose sensor based on NiO hollow spheres. Electrochim. Acta. **102**, 104–107 (2013)

32. Z. Zhuang, X. Su, H. Yuan, Q. Sun, D. Xiao, M.M.F. Choi, An improved sensitivity non-enzymatic glucose sensor based on a CuO nanowire modified Cu electrode. Analyst. **133**, 126–132 (2008)

33. M. Wang, M. Shi, E. Meng, F. Gong, F. Li, Non-enzymatic glucose sensor based on three-dimensional hierarchical Co_3O_4 nanobooks. Micro Nano Lett. **15**, 193–197 (2020)

34. M. Hilal, J. In Han, Facile preparation of three-dimensional hierarchical MgO microstructures for non-enzymatic glucose sensor. Appl. Surf. Sci. **619**, 156750 (2023)

35. W.T. Chiu, T.F.M. Chang, M. Sone, A. Tixier-Mita, H. Toshiyosh, Roles of TiO_2 in the highly robust Au nanoparticles-TiO_2 modified polyaniline electrode towards non-enzymatic sensing of glucose. Talanta, **212**, 120780 (2020)

36. Q. Dong, D. Song, Y. Huang, Z. Xu, J. H. Chapman, W.S. Willis, B. Li, Y. Lei, High-temperature annealing enabled iridium oxide nanofibers for both non-enzymatic glucose and solid-state pH sensing. Electrochim. Acta. **281**, 117–126 (2018)

37. Y. Myung, D.M. Jang, Y.J. Cho, H.S. Kim, J. Park, J-U. Kim, Y. Choi, C.J. Lee, Nonenzymatic amperometric glucose sensing of platinum, copper sulfide, and tin oxide nanoparticle-carbon nanotube hybrid nanostructures, J. Phys. Chem. C. **113**, 1251–1259 (2009)

38. L. Chen, X. Xu, F. Cui, Q. Qiu, X. Chen, J. Xu, Au nanoparticles-ZnO composite nanotubes using natural silk fibroin fiber as template for electrochemical non-enzymatic sensing of hydrogen peroxide. Anal. Biochem. **554**, 1–8 (2018)

39. Q. Dong, H. Ryu, Y. Lei, Metal oxide based non-enzymatic electrochemical sensors for glucose detection. Electrochim. Acta. **370**, 137744 (2021)

40. A. Hastir, N. Kohli, R.C. Singh, Comparative study on gas sensing properties of rare earth (Tb, Dy and Er) doped ZnO sensor. J. Phys. Chem. **105**, 23–34 (2017)

41. K. Kasirajan, L.B. Chandrasekar, S. Maheswari, M. Karunakaran, P.S. Sundaram, A comparative study of different rare-earth (Gd, Nd, and Sm) metals doped ZnO thin films and its room temperature ammonia gas sensor activity: Synthesis, characterization, and investigation on the impact of dopant. Opt. Mater. (Amst). **121**, 111554 (2021)

42. B. Renganathan, S.K. Rao, M.S. Kamath, K. Ajitha, A.R. Ganesan, A. Deepak, Performance evaluation of Ce doped ZnO clad modified fiber optic non-enzymatic glucose

electrochemical sensor based on multilayer Ti_3C_2 MXene, graphitized multi-walled carbon nanotubes and ZnO nanospheres. Microchem. J. **178**, 107410 (2022)

sensor at varying ambient temperatures for blood sugar detection applications. Microchem. J. **183**, 107890 (2022)

43. D. Kumar, A. Dwivedi, M. Srivastava, A. Srivastava, A. Srivastava, S.K. Srivastava, Gold nanorods modified Eu:Y_2O_3 dispersed PVA film as a highly sensitive plasmon-enhanced luminescence probe for excellent and fast non-enzymatic detection of H_2O_2 and glucose. Optik. **228**, 166130 (2021)

44. A. Manikandan, E. Manikandan, B. Meenatchi, S. Vadivel, S.K. Jaganathan, R. Ladchumananandasivam, M. Henin, M. Maaza, J.S. Aanand, Rare earth element (REE) lanthanum doped zinc oxide (La: ZnO) nanomaterials: Synthesis structural optical and antibacterial studies. J. Alloys Compd. **723**, 1155–1161 (2017)

45. N. Dhanalakshmi, T. Priya, N. Thinakaran, Highly electroactive Ce-ZnO/rGO nanocomposite: ultra-sensitive electrochemical sensing platform for carbamazepine determination. J. Electroanal. Chem. **826**, 150–156 (2018)

46. A. Mahmoud, M. Echabaane, K. Omri, J. Boudon, L. Saviot, N. Millot, R.B. Chaabane, Cu-doped ZnO nanoparticles for non-enzymatic glucose sensing. Molecules. **26**, 929 (2021)

47. R. Bomila, S. Srinivasan, S. Gunasekaran, A. Manikandan, Enhanced photocatalytic degradation of methylene blue dye, opto-magnetic and antibacterial behaviour of pure and La-doped ZnO nanoparticles. J. Supercond. Nov. Magn. **31**, 855–864 (2018)

48. A. Mostafaei, A. Zolriasatein, Synthesis and characterization of conducting polyaniline nanocomposites containing ZnO nanorods. Prog. Nat. Sci. Mater. Int. **22**, 273–280 (2012)

49. M.V. Kulkarni, A.K. Viswanath, R. Marimuthu, T. Seth, Synthesis and characterization of polyaniline doped with organic acids. J. Polym. Sci. **42**, 2043–2049 (2004)

50. M. Trchová, I. Šeděnková, E. Tobolková, J. Stejskal, FTIR spectroscopic and conductivity study of the thermal degradation of polyaniline films, Polym. Degrad. Stab. **86**, 179–185 (2004)

51. Y. Zhang, J. Liu, Y. Zhang, J. Liu, Y. Duan, Facile synthesis of hierarchical nanocomposites of aligned polyaniline nanorods on reduced graphene oxide nanosheets for microwave absorbing materials. RSC Adv. **7**, 54031–54038 (2017)

52. A. Abdolahi, E. Hamzah, Z. Ibrahim, S. Hashim, Synthesis of uniform polyaniline nanofibers through interfacial polymerization. Materials. **5**, 1487–1494 (2012)

53. Z.R. Khan, M.S. Khan, M. Zulfequar, M.S. Khan, Optical and structural properties of ZnO thin films fabricated by sol-gel method. Mater. Sci. Appl. **2**, 340–345 (2011)

54. A. Roychoudhury, S. Basu, S.K. Jha, Dopamine biosensor based on surface functionalized nanostructured nickel oxide platform. Biosens. Bioelectron. **84**, 72–81 (2016)

55. V.S. Jamadade, D.S. Dhawale, C.D. Lokhande, Studies on electrosynthesized leucoemeraldine, emeraldine and pernigraniline forms of polyaniline films and their supercapacitive behavior, Synth. Met. **160**, 955–960 (2010). https://doi.org/10.1016/j.synthmet.2010.02.00

56. S. Senthilkumaar, K. Rajendran, S. Banerjee, T.K. Chini, V. Sengodan, Influence of Mn doping on the microstructure and optical property of ZnO. Mater. Sci. Semicond. Process. **11**, 6–12 (2008)

57. G. Baytemir, N. Taşaltın, B. Karaca, S. Karakuş, G. Gürsu, B. Barış, D.E. Yıldız, PANI: silicene nanocomposites based non-enzymatic electrochemical voltammetric sensor for dopamine detection. J. Mater. Sci.: Mater. Electron. **34**(17), 1374–1394 (2023)

58. D.E. Yildiz, G. Baytemir, N. Taşaltın, S. Karakuş, G. Gürsu, D.A. Kose, Ni (Leu). Based Non-Enzymatic Electrochem. Dopamine Sens. Phys. Scripta. **98**, 125906 (2023)

59. Impedance, Spectroscopy, (2005). https://doi.org/10.1002/0471716243.fmatter

60. C. Zhai, D. Gan, G. Hanaor, Proust, Stress-dependent electrical transport and its universal scaling in granular materials. Extrem. Mech. Lett. **22**, 83–88 (2018)

61. E. von Hauff, Impedance spectroscopy for emerging photovoltaics. Phys. Chem. **C**, 123, 11329–11346 (2019)

62. A. Turut, D.E. Yıldız, A. Karabulut, I. Orak, Electrical characteristics of atomic layer deposited Au/Ti/HfO2/n-GaAs MIS diodes in the wide temperature range. J. Mater. Sci.: Mater. Electron. **31**, 7839–7849 (2020)

63. J.R. Jennings, Y. Liu, F. Safari-Alamuti, Q. Wang, Dependence of dye-sensitized solar cell impedance on photoelectrode thickness. J. Phys. Chem. C **116**, 1556–1562 (2012)

64. D.E. Yıldız, D. Cevher, M. Yasa, A. Cirpan, L. Toppare, Selenophene-containing conjugated polymers for supercapacitor electrodes. J. Polym. Sci. **60**, 109–121 (2022)

65. O. Polat, M. Coskun, P. Roupcova, D. Sobola, Z. Durmus, M. Caglar, T. Sikola, A. Turut, Influence of iridium (ir) doping on the structural, electrical, and dielectric properties of LuFeO3 perovskite compound. J. Alloys Compd. **877**, 160282 (2021)

66. M. Coşkun, A.O. Polat, F.M. Coşkun, Z. Durmuş, C.M. Caglar, A. Türüt, The electrical modulus and other dielectric properties by the impedance spectroscopy of $LaCrO_3$ and LaCr0.90Ir0.10O3 perovskites. RSC Adv. **8**, 4634–4648 (2018)

67. D.E. Yıldız, A. Karabulut, I. Orak, A. Turut, Effect of atomic-layer-deposited HfO2 thin-film interfacial layer on

the electrical properties of Au/Ti/n-GaAs Schottky diode. J. Mater. Sci.: Mater. Electron. **32**, 10209–10223 (2021)

68. A.M. Nawar, M.M. Makhlouf, Au-nanoparticles doped SiO2 interfacial layer to promote the photovoltaic characteristics of Au/p-Si/Al solar cells. J. Alloys Compd. **767**, 1271–1281 (2018)

69. D.E. Yıldız, A. Tataroglu, Analysis of dielectric, impedance and electrical properties of interfacial layer: AlN. J. Mater. Sci.: Mater. Electron. **34**(12), 1057 (2023)

70. K. Sambasiva Rao, D. Madhava Prasad, P. Murali Krishna, B. Tilak, K.C. Varadarajulu, Impedance and modulus spectroscopy studies on $Ba_{0.1}Sr_{0.81}La_{0.06}Bi_2Nb_2O_9$ ceramic. Mater. Sci. Engineering: B **133**, 141–150 (2006)

71. N. Channa, M. Khalid, A.D. Chandio, M.S. Akhtar, J.K. Khan, G. Mustafa, Z.A. Muniba, Gilani, Structural, dielectric, impedance, and electric modulus properties of Cu^{2+}substituted $Cu_xMn_{1-x}Fe_2O_4$ spinel ferrites nanoparticles. J. Mater. Sci.: Mater. Electron. **32**, 2832–2844 (2021)

72. F. Kremer, A. Schönhals, B.D. Spectroscopy (eds.), (2003). https://doi.org/10.1007/978-3-642-56120-7

73. S. Karadeniz, D.E. Yıldız, Frequency dependent dielectric spectroscopy of Au/n-Si structure with stannic oxide (SnO_2) interfacial layer. J. Mater. Sci.: Mater. Electron. **34**, 1–12 (2023)

74. H.H. Gullu, D.E. Yildiz, Temperature and frequency effects on electrical and dielectric properties of n-4H SiC based metal–insulator-semiconductor (MIS) diode interlayered with Si_3N_4 thin film. J. Mater. Sci.: Mater. Electron. **31**, 8705–8717 (2020)

75. N. Maouche, B. Nessark, Cyclic Voltammetry and Impedance Spectroscopy Behavior Studies of Polyterthiophene Modified Electrode. Int. J. Electrochem. **2011**, 1–5 (2011)

76. R. Inada, S. Yasuda, H. Hosokawa, M. Saito, T. Tojo, Y. Sakurai, Formation and Stability of Interface between Garnet-Type Ta-doped $Li_7La_3Zr_2O_{12}$ Solid Electrolyte and Lithium Metal Electrode. Batteries **4**(4), 26 (2018). https://doi.org/10.3390/BATTERIES4020026

77. C. Ratlam, S. Phanichphant, S. Sriwichai, Development of dopamine biosensor based on polyaniline/carbon quantum dots composite. J. Polym. Res. **27**, 183 (2020)

78. W.-F. Hsu, T.-M. Wu, Electrochemical sensor based on conductive polyaniline coated hollow tin oxide nanoparticles and nitrogen doped graphene quantum dots for sensitively detecting dopamine. J. Mater. Sci. : Mater. Electron. **30**, 8449–8456 (2019)

79. L.-Q. Xie, Y.-H. Zhang, F. Gao, Q.-A. Wu, P.-Y. Xu, S.-S. Wang, N.-N. Gao, Q.-X. Wang, A highly sensitive dopamine sensor based on a polyaniline/reduced graphene oxide/Nafon nanocomposite. Chin. Chem. Lett. **28**, 41–48 (2017)

80. J. Mathiyarasu, S. Senthilkumar, K.L.N. Phani, V. Yegnaraman, Selective detection of dopamine using a functionalised polyaniline composite electrode. J. Appl. Electrochem. **35**, 513–519 (2005)

Publisher's Note   Springer Nature remains neutral with regard to jurisdictional claims in published maps and institutional affiliations.